

Single-chain antibody fragments derived from a human synthetic phage-display library bind thrombospondin and inhibit sickle cell adhesion

Nicholas A. Watkins, Lily M. Du, J. Paul Scott, Willem H. Ouwehand, and Cheryl A. Hillery

The enhanced adhesion of sickle red blood cells (RBCs) to the vascular endothelium and subendothelial matrix likely plays a significant role in the pathogenesis of vaso-occlusion in sickle cell disease. Sickle RBCs have enhanced adhesion to the plasma and extracellular matrix protein thrombospondin-1 (TSP) under conditions of flow *in vitro*. In this study, we sought to develop antibodies that bind TSP from a highly diverse library of human single-chain Fv fragments (scFvs) displayed on filamentous phage. Following 3 rounds of phage selection of increas-

ing stringency 6 unique scFvs that bound purified TSP by enzyme-linked immunosorbent assay were isolated. Using an *in vitro* flow adhesion assay, 3 of the 6 isolated scFvs inhibited the adhesion of sickle RBCs to immobilized TSP by more than 40% compared with control scFvs ($P < .001$). Furthermore, scFv TSP-A10 partially inhibited sickle RBC adhesion to activated endothelial cells ($P < .005$). Using TSP proteolytic fragments to map the binding site, we showed that 2 of the inhibitory scFvs bound an epitope in the calcium-binding domain or proximal cell-

binding domain of TSP, providing evidence for the role of these domains in the adhesion of sickle RBCs to TSP. In summary, we have isolated a panel of scFvs that specifically bind to TSP and differentially inhibit sickle RBC adhesion to surface-bound TSP under flow conditions. These scFvs will be useful reagents for investigating the role of the calcium and cell-binding domains of TSP in sickle RBC adhesion. (Blood. 2003;102:718-724)

© 2003 by The American Society of Hematology

Introduction

The major cause of morbidity and mortality in sickle cell disease is tissue ischemia and infarction due to vascular occlusion. The pathogenesis of vaso-occlusion remains unclear and likely involves many complex steps related to both the primary event of deoxyhemoglobin S polymerization and the many resultant pathologic changes in both the sickle erythrocyte and the vascular endothelium.¹ The increased adhesion of sickle red blood cells (RBCs) to vascular endothelium through multiple adhesive pathways likely contributes to the pathogenesis of vaso-occlusion in sickle cell disease.²⁻⁷ For example, sickle RBCs can bind directly to the plasma and extracellular matrix protein thrombospondin-1 (TSP)^{8,9} as well as to cultured endothelial cells via a TSP-dependent pathway.^{10,11} Additionally, sickle RBCs bind to TSP in the subendothelial matrix exposed between thrombin-stimulated endothelial cells.¹² In agreement, the addition of TSP increases sickle RBC adhesion to the rat mesoceleal microcirculation *ex vivo*.¹³ Finally, Browne et al¹⁴ found that levels of circulating plasma TSP significantly increase in patients with sickle cell disease during crisis to concentrations that can support maximal sickle RBC adhesion to endothelial cells *in vitro*.

The exact site on TSP that binds sickle RBCs is not known. We found that digestion of the carboxy-terminal cell-binding domain of TSP (TSP-CBD), which is adjacent to the calcium-binding domain, fully disrupts sickle RBC adhesion to surface-bound TSP.¹⁵ However, monoclonal antibody (mAb) C6.7,

which binds the TSP-CBD and blocks platelet and melanoma cell adhesion to TSP,^{16,17} does not inhibit sickle RBC adhesion to TSP.¹⁵ Additionally, adhesive peptides from the TSP-CBD that inhibit as well as support TSP-mediated adhesion of platelets and transformed cells¹⁸ failed to either inhibit or support sickle RBC adhesion to TSP within our experimental model.¹⁵ This suggests that sickle RBCs may bind to a unique adhesive site within the TSP-CBD that is exposed after TSP binds to a matrix.

That the exact site on TSP that binds sickle RBCs is not known has hampered attempts to develop reagents that effectively inhibit sickle RBC adhesion to TSP. Therefore, in this study, we sought to develop reagents that bind TSP and inhibit sickle RBC adhesion using a highly diverse library of human single-chain variable domain antibody fragments (scFvs) displayed on the surface of filamentous bacteriophage.¹⁹ This library is composed of the complete repertoire of human germ-line heavy and light chain variable genes (VH and VL, respectively), to which random nucleotide sequences of variable length have been appended to introduce coding sequence for the third complementarity determining regions (CDR3s).²⁰ The repertoire of synthetic VH and VL domains can be expressed on the surface of filamentous bacteriophage, permitting the isolation of scFvs with desired specificities. This library was selected on purified TSP and screened for scFvs that inhibited the binding of sickle RBCs to TSP.

From the Department of Pediatrics, Medical College of Wisconsin, Milwaukee, WI; the Blood Research Institute, the Blood Center of Southeastern Wisconsin, Milwaukee, WI; and the Department of Haematology, University of Cambridge and National Blood Service, Cambridge, United Kingdom.

Submitted November 19, 2002; accepted March 20, 2003. Prepublished online as *Blood* First Edition Paper, March 27, 2003; DOI 10.1182/blood-2002-11-3497.

Supported by American Heart Association Grant-in-Aid 0050467N (C.A.H.), Public Health Services grant HL70981 and HL44612 (C.A.H.), and General

Clinical Research Center grant M01-RR00058 from the National Institutes of Health.

Reprints: Cheryl A. Hillery, Medical College of Wisconsin and Blood Research Institute, PO Box 2178, Milwaukee, WI 53201-2178; e-mail: chillery@bcsew.edu.

The publication costs of this article were defrayed in part by page charge payment. Therefore, and solely to indicate this fact, this article is hereby marked "advertisement" in accordance with 18 U.S.C. section 1734.

© 2003 by The American Society of Hematology

Materials and methods

The Griffin.1 library

The Griffin.1 library is composed of human scFvs containing highly diverse CDR3s in both the VH and VL domains. This library was derived by recloning VH and VL from human synthetic Fab lox library vectors²⁰ into the phagemid vector pHEN2.²¹ ScFvs can be displayed on the surface of bacteriophage when expressed in suppressor *Escherichia coli* strains (eg, TG1) or as soluble fragments that also contain the c-myc tag and carboxy-terminus His-tag in nonsuppressor *E coli* strains (eg, HB2151).

Selection of TSP-specific scFvs

Phage particles expressing scFv were prepared as previously described.²² TSP, purified from human platelet releasate^{15,23} and diluted in carbonate buffer, was coated (10 µg/mL) on Maxisorp immunotubes (Nunc, Rochester, NY) overnight at 4°C. The tubes were then blocked with phosphate-buffered saline (PBS) containing 2% dry milk (MPBS), and approximately 10¹⁴ phage in 4 mL MPBS was incubated with the TSP-coated immunotube for 120 minutes at room temperature. After washing 10 times with PBS containing 0.1% Tween 20 and 10 times with PBS, bound phage were eluted with 100 mM triethylamine, neutralized with 1 M Tris (tris(hydroxymethyl)aminomethane; pH 7.4), and used to infect *E coli*. Infected bacteria were plated on tryptone yeast extract agar (TYE) containing 1% glucose and 100 µg/mL ampicillin in a BioAssay dish (Nunc) and grown overnight at 30°C. An aliquot of the BioAssay dish bacterial lawn was used to produce phage for additional rounds of selection.²² A total of 3 rounds of selection were performed under increasingly stringent conditions to augment the specificity and affinity of selected bound phage. The immunotubes were washed 40 times in round 2 and 60 times in round 3.

Screening of selected clones

Following each round of selection, the HB2151 nonsuppressor strain of *E coli* was infected with an aliquot of eluted phage in order to allow expression of soluble scFv. From each round, 96 random colonies were picked and scFv expression was induced with isopropyl beta-D-galactopyranoside as previously described.²² Following overnight expression, the scFvs were screened for binding to TSP by enzyme-linked immunosorbent assay (ELISA). Bacterial supernatant (100 µL) containing expressed scFv was incubated for one hour at room temperature in microtiter wells that had been coated with TSP (10 µg/mL TSP in carbonate buffer, 50 µL/well, 4°C overnight) and blocked with bovine serum albumin (BSA; 2% BSA in PBS, 2 hours at room temperature). The wells were washed 3 times and bound scFv detected with mAb 9E10 (4 µg/mL in PBS/1% BSA), followed by horseradish peroxidase (HRP)-conjugated goat anti-mouse immunoglobulin G (IgG; Fc specific, 1:500). The mAb 9E10 recognizes the c-myc tag, which is expressed at the carboxy-terminus of all scFvs.²⁴ Immune complexes were detected with 3,3',5,5'-tetramethylbenzidine (Sigma, St Louis, MO).

TSP-specific scFvs were purified by means of the carboxy-terminus His-tag using a Talon metal affinity column as directed by the manufacturer (Clontech, Palo Alto, CA).

DNA sequencing

Phagemid DNA was isolated from 2 mL overnight cultures of TSP-specific clones using Qiagen Miniprep kit according to the manufacturer's instructions (Valencia, CA). The nucleotide sequence of the VH and VL genes of selected clones was determined using the primers FOR_LinkSeq (GCCACCTCCGCTGAACC) and pHEN-SEQ (CTATGCGCCCCAT-TCA) using dye terminator chemistry (ABI Ready Reaction mixture; Applied Biosystems, Foster City, CA). The nucleotide sequences obtained were compared with germ-line V gene sequences using the online Vbase directory.²⁵

Immunoblot analysis and TSP digestion

Purified TSP (2 µg/lane) was resolved by sodium dodecyl sulfate-polyacrylamide gel electrophoresis (SDS-PAGE) under reducing conditions, transferred to polyvinylidene fluoride (PVDF) membrane, blocked with 3% gelatin (one hour, 37°C), and incubated with bacterial supernatants containing expressed scFv (4°C, overnight). Bound scFv was incubated with mAb 9E10 (10 µg/mL), followed by alkaline phosphatase-conjugated goat anti-mouse IgG (1:3000). Immune complexes were detected using ImmunoPure NBT/BCIP Substrate kit according to the manufacturer's instructions (Pierce, Rockford, IL). Rabbit polyclonal anti-TSP-CBD (Cell-5, kindly provided by Dr William Frazier, Washington University) was used for a positive control and was detected with alkaline phosphatase-conjugated goat anti-rabbit IgG.

TSP in Tris-buffered saline (TBS, 20 mM Tris-HCl, pH 7.4, 150 mM NaCl) was digested with thermolysin (1:100, wt/wt) in the presence of 1 mM CaCl₂ (40 minutes) or chymotrypsin (1:100, wt/wt) in the presence of 1 mM CaCl₂ (60 minutes) or 10 mM EDTA (ethylenediaminetetraacetic acid; 35 minutes) at room temperature as previously described.^{15,26-28} The reactions were stopped by boiling in 4X NuPAGE lithium dodecylsulfate sample buffer (Invitrogen, Carlsbad, CA) for 5 minutes. Digested TSP (3 µg/lane) was resolved using 4% to 12% NuPAGE Bis-Tris Gel with or without reduction using NuPAGE 10X Reducing Agent following the manufacturer's guidelines (Invitrogen). The gels were either stained with Coomassie blue or transferred to PVDF membrane and blocked with MPBS (5% dried milk, room temperature, overnight). Following incubation with bacterial supernatants containing expressed scFv (3 hours, 37°C), bound scFv was detected with mAb 9E10 (10 µg/mL in 2% MPBS), followed by HRP-conjugated goat anti-mouse IgG (1:1000 in 2% MPBS). Immune complexes were detected by fluorescent exposure of autoradiography film using enhanced chemiluminescence Western blotting detection kit (Amersham, Arlington Heights, IL).

Blood preparation and flow adhesion assay

Approval for these studies was obtained from the Children's Hospital of Wisconsin institutional review board. After obtaining informed consent, blood samples were collected from patients with homozygous sickle cell disease (hemoglobin SS) in 3.8% sodium citrate (vol, 1:9). The RBCs were washed 3 times and resuspended at a 2% hematocrit in M199 serum-free cell culture medium (Sigma) containing 0.2% bovine serum albumin (SFM-BSA) as previously described.⁸ Sickle RBC adhesion was studied using a parallel plate perfusion chamber on an inverted phase microscope at 37°C as previously described.⁸ In brief, purified TSP was coated on a 35-mm² tissue culture plate (2 µg/cm², 60 minutes, 37°C), followed by an incubation with 2% BSA in TBS with 1 mM CaCl₂ to block the surface. Following insertion of a gasket and the flow chamber, the wells were rinsed for a period of 3 to 5 minutes with SFM-BSA. Washed RBCs were perfused through the chamber at a wall shear stress of 1 dyne/cm². Following a 5-minute rinse period, the number of adherent RBCs was counted by direct microscopic visualization of 4 random fields/well in duplicate wells. For inhibition experiments, bacterial supernatant containing the expressed scFv being tested was incubated with the coated and blocked surface for 30 minutes at 37°C prior to the initiation of the flow adhesion assay.

For the endothelial cell adhesion assays, human umbilical endothelial cells (HUVECs) were isolated from anonymous umbilical cords, obtained in accordance with established institutional guidelines, and grown as previously described.²⁹ Third-passage HUVECs, grown to confluence on gelatin-coated 35-mm² tissue culture plates, were treated for 4 to 8 hours with recombinant human tumor necrosis factor-α (500 U/mL or 5.5 ng/mL; Sigma)³⁰ and interleukin-1β (50 pg/mL; Peprotech, Rocky Hill, NJ)^{31,32} prior to the flow adhesion assay. The cytokine-treated HUVEC monolayer was placed into the flow chamber, rinsed briefly with SFM-BSA, and then incubated with SFM-BSA or 5 µg/mL TSP in SFM-BSA for 20 minutes at 37°C under static conditions. Washed RBCs (2% hematocrit in 3 mL SFM-BSA) or heparinized whole blood (20 U/mL heparin, 1 mL total volume) were perfused through the chambers and rinsed, and adherent RBCs were counted as described in the previous paragraph.

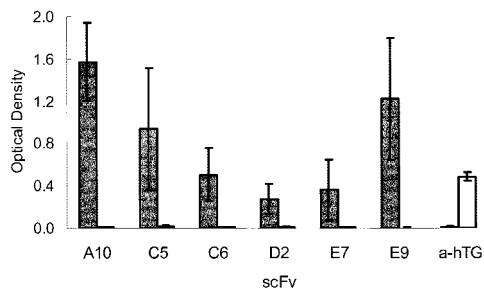


Figure 1. scFvs specifically bind TSP. Bacterial supernatants containing expressed soluble scFv (TSP-A10, -C5, -C6, -D2, -E7, -E9, or anti-human thyroglobulin (a-hTG) control scFv that binds hTG) were incubated in microtiter wells coated with 0.5 μ g/well of purified human TSP-1 (TSP, \blacksquare) or control protein hTG (\square). Bound scFvs were detected by ELISA using anti-c-myc mAb 9E10 as described in "Materials and methods." The graph depicts the means \pm SEs of 4 experiments.

Resonant mirror biosensor measurement of scFv binding to TSP

The affinity of selected scFvs for TSP was determined using an IAsys auto+ affinity sensor (Affinity Sensors, Cambridge, United Kingdom). Purified TSP was immobilized onto the surface of a carboxymethyl-dextran cuvette following the manufacturer's instructions. The binding of purified scFv TSP-A10 was then detected over a 7 to 0.1 μ M concentration range. The dissociation constant (K_d) of TSP-A10 was determined on 3 separate occasions using the IAsys Affinity Sensor and proprietary software from IAsys (FastFit). The final value reported is an average of the 3 measurements.

Statistical analysis

Data were analyzed by the 2-sample Student *t* test in which a 2-tail *P* value less than .05 was considered statistically significant.

Results

Selection of TSP-specific scFvs

Phagemid particles displaying scFvs from the *Griffin.1* library²⁰ that bound purified TSP were isolated following 3 rounds of phage

selection as described.²² Soluble scFv expressed from 96 random clones from the second and third rounds of selection was screened for binding to TSP by ELISA. A total of 6 unique scFvs specific for TSP were selected for further characterization (Figure 1).

Immunoblot analysis of scFv with TSP proteolytic fragments

While all scFvs bound native TSP in ELISA (Figure 1), only scFvs TSP-A10, TSP-C6, TSP-D2, and TSP-E9 bound denatured TSP resolved by SDS-PAGE with TSP-A10 and TSP-E9 recognizing both reduced and nonreduced TSP (Figure 2A). To further define the region of TSP that these scFvs bound, several strategies were used to generate proteolytic fragments of TSP. Thermolysin digestion of TSP in the presence of calcium generates a 25-kDa fragment that contains the amino-terminal heparin-binding domain, and a 140-kDa carboxy-terminal proteolytic fragment (Figure 2B).²⁶ Chymotrypsin digestion of TSP in the presence of EDTA produces a 70-kDa TSP fragment that contains the type 1 and type 2 repeats. Alternatively, chymotrypsin digestion of TSP in the presence of calcium, which protects the Ca^{++} -binding domain from proteolytic cleavage, yields a 120-kDa carboxy-terminal proteolytic fragment that is similar to the 140-kDa fragment except for loss of the final 18 to 20 kDa of the carboxy-terminal portion of the TSP-CBD.²⁷ The approximate locations of the 25-kDa, 140-kDa, 120-kDa, and 70-kDa proteolytic fragments as identified by amino-terminal sequencing and size^{17,26,28,33} are shown in Figure 2B.

As shown in Figure 2C-D, the scFv clone TSP-A10 bound both reduced and nonreduced 140-kDa and 120-kDa TSP fragments, but not the more amino-terminal 25-kDa and 70-kDa fragments. A similar pattern was seen for the scFv clone TSP-E9, suggesting that the binding sites for these 2 scFvs are located in the Ca^{++} -binding domain or a proximal portion of the TSP-CBD. The scFv clones TSP-C6 and TSP-D2, which recognized only *nonreduced* intact TSP (Figure 2A), both bound the 70-kDa TSP fragment in addition to the 140-kDa and 120-kDa TSP fragments under nonreducing conditions (Figure 2D). This suggests that both TSP-C6 and TSP-D2 bind to the more central region of TSP. The scFv clones

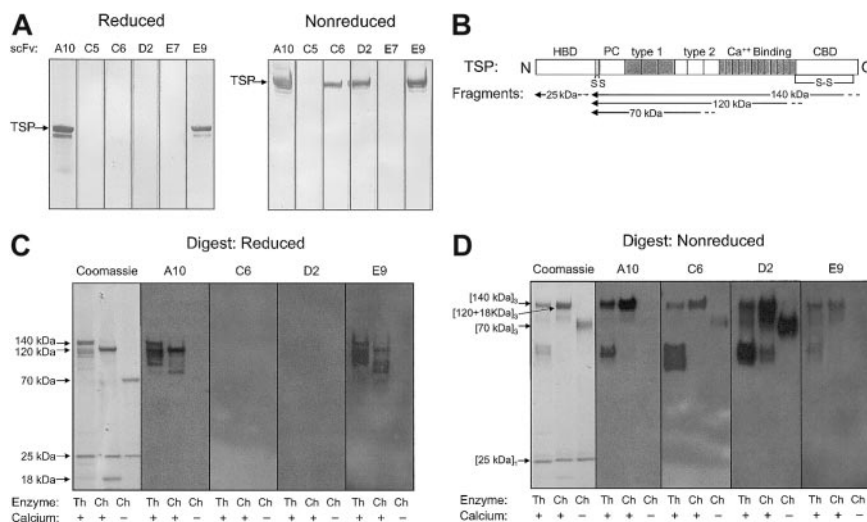


Figure 2. Immunoblot of selected scFvs with purified intact TSP and TSP digests. Bacterial supernatants containing expressed soluble scFv (TSP-A10, -C5, -C6, -D2, -E7, and -E9) were incubated with (A) purified human platelet TSP or (C-D) TSP digested with thermolysin in the presence of $CaCl_2$ (Th/+), chymotrypsin in the presence of $CaCl_2$ (Ch/+), or chymotrypsin in the presence of EDTA (Ch/-) resolved by PAGE under reducing (A,C) or nonreducing (D) conditions and transferred to PVDF membrane. Bound scFv was detected by anti-c-myc mAb 9E10 as described in "Materials and methods." (B) Schematic illustration of TSP monomer with selected domains as described in the text. HBD indicates heparin-binding domain; PC, procollagen-like region; type 1, type 1 repeats; type 2, type 2 repeats; Ca^{++} Binding, Ca^{++} -binding domains or type 3 repeats; CBD, cell-binding domain; S, site of cysteines that disulfide link TSP chains to form trimer; and S-S, disulfide bond in C-terminal region. The approximate locations of the 25-kDa, 140-kDa, 120-kDa, 18-kDa, and 70-kDa proteolytic fragments as identified by amino-terminal sequencing and size^{26,28,33} are indicated by arrows. The 25-kDa fragment is a monomer,²⁶ the 70-kDa, 120-kDa, and 140-kDa fragments are trimers,³³ and the 18- to 20-kDa C-terminal fragment remains disulfide linked to the 120-kDa fragment.¹⁷

TSP-C5 and TSP-E7 did not bind full-length or digested TSP under either reducing or nonreducing SDS-PAGE conditions (Figure 2A and data not shown). This suggests that the epitopes recognized by these 2 scFv Abs are destroyed when TSP is denatured.

Effect of scFv on sickle RBC adhesion to TSP

Sickle RBCs avidly bind immobilized TSP under flow conditions.^{8,10,11} To date, multiple, well-characterized TSP-specific mAbs do not inhibit sickle RBC adhesion within our experimental model.^{8,15} Therefore, the selected scFvs were tested for their ability to inhibit sickle RBC adhesion. Bacterial supernatants containing soluble scFv were incubated with TSP immobilized on the surface of a parallel plate flow adhesion assay. Washed sickle RBCs were then perfused over the treated TSP at a wall shear stress of 1 dyne/cm², a force similar to that found in postcapillary venules, a proposed site of vascular obstruction in sickle cell disease.^{5,34} Bacterial supernatants containing clones TSP-A10, TSP-C5, and TSP-E9 inhibited sickle RBC adhesion to TSP compared with bacterial supernatants containing a control (anti-human thyroglobulin; a-hTG) scFv (Figure 3, *P* < .001). In contrast, scFv clones TSP-C6, TSP-D2, and TSP-E7 did not inhibit sickle RBC adhesion compared with the control scFv (Figure 3). Of note, bacterial supernatant containing the control scFv directed against human thyroglobulin that does not bind native TSP (Figure 1, a-hTG) modestly inhibited sickle RBC adhesion compared with buffer control (76% RBC adhesion, *P* = .03), showing a mild nonspecific effect likely due to the bacterial supernatant.

Effect of purified scFv on sickle RBC adhesion to TSP

To characterize this inhibition further, scFv TSP-A10 was expressed and purified by Talon affinity chromatography. When the purified scFv was incubated with TSP and included during the RBC perfusion (10 μg/mL), TSP-A10 consistently inhibited the adhesion of sickle RBCs to immobilized TSP by approximately 40% (Figure 4, *P* = .0002). This inhibition required the inclusion of scFv throughout the experiment. If the flow chamber was rinsed prior to the RBC perfusion, the effect on RBC adhesion was modest and variable (data not shown). This suggests that scFv TSP-A10 has a relatively low affinity. In agreement, kinetic studies found that scFv TSP-A10 bound purified TSP with a *K_d* of approximately 2 μM (data not shown). The use of purified scFv reduced the nonspecific inhibition that was seen when bacterial supernatant was used (Figures 3-4).

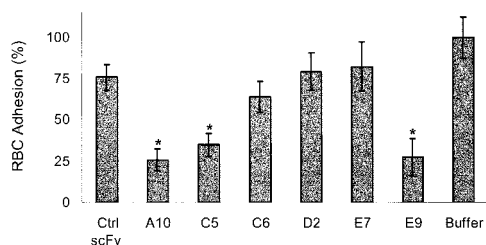


Figure 3. Effect of scFv on sickle RBC adhesion to immobilized TSP. Parallel plate flow chambers were coated with purified TSP (2 μg/cm²), blocked with 2% BSA, and incubated with bacterial supernatants containing scFv. Control scFv (Ctrl scFv [a-hTG], n = 12), TSP-A10 (A10, n = 6), TSP-C5 (C5, n = 6), TSP-C6 (C6, n = 6), TSP-D2 (D2, n = 7), TSP-E7 (E7, n = 6), TSP-E9 (E9, n = 7), or control buffer (buffer, n = 19). Washed sickle RBCs were perfused through flow chambers at a wall shear stress of 1 dyne/cm² as described in "Materials and methods." After rinsing, adherent RBCs per unit area were counted by direct microscopic visualization. The results are shown as the means ± SEs of sickle RBC adhesion, normalized to sickle RBC adhesion to buffer-treated TSP (900 ± 110 RBCs/mm², n = 19). The * indicates a *P* value of .001 or less compared with control scFv.

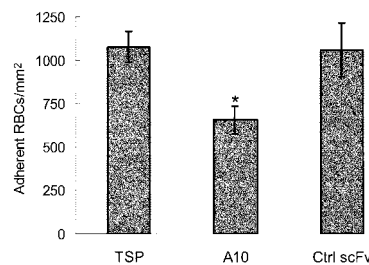


Figure 4. Sickle RBC adhesion to TSP is inhibited by the purified scFv TSP-A10. Washed sickle RBCs and TSP immobilized on perfusion chamber wells were incubated with control buffer (TSP), purified scFv TSP-A10 (10 μg/mL, n = 10), or purified control scFv (a-hTG; 10 μg/mL, n = 6) for 60 minutes at room temperature. Treated RBCs were perfused through flow chambers at a wall shear stress of 1 dyne/cm², and adherent cells were counted as described in Figure 3. The results are shown as the means ± SEs of adherent RBCs/mm². The * indicates a *P* value of .0002 or less compared with control scFv.

Effect of scFv TSP-A10 on sickle RBC adhesion to activated endothelial cells

In order to determine whether the scFv TSP-A10 affected sickle RBC adhesion under more physiologic conditions, we incubated cytokine-stimulated endothelial cells with TSP-A10 followed by perfusion of washed sickle RBCs through the flow chamber. As shown in Figure 5, there was no effect of TSP-A10 on sickle RBC adhesion to activated endothelial cells until TSP was also added to the experimental system. This suggests that TSP-A10 is specific for inhibiting sickle RBC adhesion to endothelial cells via TSP-dependent mechanisms. Interestingly, when whole blood was perfused over activated endothelial cells preincubated with TSP, there was a significant increase in overall adhesion that was only partially inhibited by TSP-A10. These data emphasize the complexity of sickle RBC adhesion and demonstrate that additional plasma and cellular factors also contribute to sickle RBC adhesion in vivo.

DNA sequence analysis of TSP binding scFv Abs

Analysis of the nucleotide sequences of the VH and VL genes of the 6 TSP-specific scFvs indicated that these clones were restricted to just 3 VH genes and 2 VL genes (Figure 6). Interestingly, the scFv clones TSP-A10 and TSP-E9, which bound the Ca⁺⁺-binding domain or proximal TSP-CBD (Figure 2C) and inhibited sickle RBC adhesion (Figure 3), use genes from different VH families, but both contained adjacent proline and arginine residues in the VH-CDR3 (Figure 6). Additionally, clones TSP-E7 and TSP-D2,

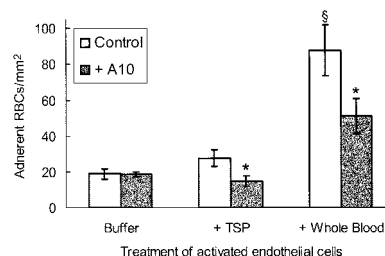


Figure 5. TSP-dependent sickle RBC adhesion to activated endothelial cells is inhibited by scFv TSP-A10. Cytokine-stimulated endothelial cells were incubated with SFM-BSA (buffer) or TSP in SFM-BSA (5 μg/mL, TSP, whole blood) with (□) or without (■) purified scFv TSP-A10 (2.3 μg/mL) for 20 minutes at 37°C as described in "Materials and methods." Washed sickle RBCs (buffer, TSP) or whole blood was perfused over the treated endothelial cells and rinsed, and adherent RBCs were counted as described in Figure 3. The results are shown as the means ± SEs of adherent RBCs/mm² (n = 3 for buffer, n = 5 for TSP and whole blood). The * indicates a *P* value less than .005 comparing TSP-A10-treated assays with control assays, and § indicates a *P* value of .01 or less comparing whole blood with either buffer or TSP under control conditions.

A Deduced amino acid sequences of the VH domains

	FR1	CDR1	FR2	CDR2	FR3	CDR3	FR4
	1 10 20 30		40	50 60	70 80 90		103
VH3-20	EVQLVESGGGVVVRPGGSLRLS	CAASGFTFD	D-YGMS	WVRQAPGKGLEWVS	GINWNGGSTGYADSVKG	RFTISRDNAKNSLYLQMN	SLRAEDTALYHCAR
TSP-A10	-----	-----	-----	-----	-----	-----V-Y-a-	LQKHPERDL WGQGTLV
VH3-23	EVQLLESVGGGLVQPGGSLRLS	CAASGFTFS	S-YAMS	WVRQAPGKGLEWVS	AISGSGGSTYYADSVKG	RFTISRDNKNTLYLQMN	SLRAEDTAVYYCAK
TSP-D2	---V-----	-----	-----	-----	-----	-----v--aR	MGTNAG WGQGTLV
TSP-E7	---V-----	-----	-----	-----	-----	-----v--aR	TIANSEV WGQGTLV
VH4-4b	QVQLQESGPGLVKPKSETLSL	CAVSGYSIS	SGYYWG	WIRQPPGKGLEWIG	SIY-HSGSTYYNPSLKS	RVTISVDTSKNQFSLKLS	SSVTAADTAVYYCAR
TSP-C5	-----	-----	-----	-----	-----	-----M--a-	GIMLSR WGQGTLV
TSP-C6	-----	-----	-----	-----	-----K-----	-----a-	GFEHQ WGQGTLV
TSP-E9	-----	-----	-----	-----	-----	-----a-	SIFRH WGQGTLV

B Deduced amino acid sequences of the VL domains

	FR1	CDR1	FR2	CDR2	FR3	CDR3	FR4
	1 10 20 30		40	50 60	70 80 90		
L11	AIQMTQSPSSLSASVGD	RVTITC	RASQGIRNDLG	WYQQKPGKAPKLLIY	AASLSQS	GVPSRFSGSGSGTDFTL	TISSLQPEDFATYYC
TSP-A10	---R-----	-----	-----	-----	-----	-----RT	FGGQTKL
1g	QSVLTQPPSASGTPGQR	VTIISC	SGSSSNIGSNYYVY	WYQQLPGTAPKLLIY	RNNQRPS	GVPDFRSGSKSGTSAS	LAIISGLRSEDEADYYC
TSP-D2	-----	-----	-----R-----	-----	-----	-----GFV	FGGQTKLTVL
TSP-E7	-----	-----	-----	-----	-----	-----GLV	FGGQTKLTVL
TSP-C5	---M--p--Y--g--	-----	-----P-----	-----	-----	-----V	FGGQTKLTVL
TSP-C6	-----	-----	-----	-----	-----	-----V	FGGQTKLTVL
TSP-E9	-----	-----	-----	-----	-----	-----V	FGGQTKLTVL

Figure 6. Deduced amino acid sequences of TSP-specific scFvs. The VH (A) and VL (B) segments of the TSP-specific scFvs were sequenced as described in "Materials and methods." The deduced amino acid sequences are shown compared with the closest germ-line V gene sequence. Homology is shown by dashed lines and silent mutations by lowercase letters, with numbering according to Kabat.⁵¹ GenBank accession numbers AF396468 to AF396479.

which did not affect sickle RBC adhesion to TSP, have VH domains derived from the heavy chain gene VH3-23 and have the nearly identical VL genes with the same VL-CDR3s. Finally, clones TSP-C5, TSP-C6, and TSP-E9 all use VH genes homologous to the VH4-4b gene and identical VL-CDR3s.

Discussion

In this study, we isolated 6 unique human scFvs with "synthetic" third CDRs that specifically bound to purified human TSP. These scFvs, which all recognize native TSP by ELISA (Figure 1), were isolated by selecting with TSP purified from platelet releasate. In immunoblotting, only TSP-A10, TSP-C6, TSP-D2, and TSP-E9 bound denatured TSP (Figure 2). Using proteolytic fragments of TSP we were able to characterize the epitopes recognized by the scFvs. TSP-C6 and TSP-D2 recognized nonreduced TSP and bound to the 70-kDa TSP fragment, signifying that these 2 scFvs likely bind an epitope within the midregion of TSP that includes the type 1 and type 2 repeats as well as the procollagen-like region (Figure 2B). While TSP-C5 and TSP-E7 bound native TSP by ELISA, they did not recognize denatured TSP by immunoblot analysis, suggesting that the essential conformational epitopes for these scFvs are lost when TSP is denatured or that the scFvs have a low affinity.

Both TSP-A10 and TSP-E9 bound an epitope on TSP present on the 120-kDa fragment, but *not* the 70-kDa amino-terminal subportion of this fragment (Figure 2). Therefore, both TSP-A10 and TSP-E9 likely recognize an epitope that derives from either the Ca⁺⁺-binding domain or a neighboring portion of the TSP-CBD. Interestingly, both scFvs also produced the greatest inhibition of sickle RBC adhesion under flow conditions (Figure 3), suggesting that there is a site within the Ca⁺⁺-binding domain or the amino portion of the TSP-CBD that interacts with sickle RBCs. In

agreement, TSP-C6 and TSP-D2, which both recognize an epitope outside of this region, had no significant effect on sickle RBC adhesion (Figure 3).

We were unable to characterize the epitope recognized by TSP-C5 and TSP-E7 by immunoblot. The former scFv showed good levels of inhibition of sickle RBC adhesion to TSP, while the latter was inert. The difference between these 2 scFvs in producing inhibition of sickle RBC adhesion implies that they either recognize different epitopes on TSP or bind with different affinities.

The serologic and functional characterization of the scFvs have interesting correlates with their deduced amino acid sequences (Figure 6). Clone TSP-A10 is derived from unique VH and VL genes (VH3-20 and VL-L11, respectively), while clone TSP-E9, with similar TSP regional binding and sickle RBC inhibition profiles, has different VH and VL genes (VH4-4b and VL-1g, respectively). Comparison of the CDR3 regions show that both TSP-A10 and TSP-E9 contain a proline adjacent to a positively charged arginine within the VH-CDR3. These may provide important conformational and/or charge properties necessary for scFv binding. Interestingly, the noninhibitory clones TSP-D2 and TSP-E7 share common VH and VL domains that are derived from the VH3-23 and VL-1g genes, respectively. Finally, clones TSP-C5, TSP-C6, and TSP-E9, which have different levels of inhibition of sickle RBC adhesion, all use the same VH and VL genes, VH4-4b and VL-1g, respectively. The observation that scFvs with highly homologous VH and VL domains may target different epitopes and that this is solely controlled by the VH-CDR3 sequence confirms earlier studies from our laboratory with scFv against the family of Rh proteins.³⁵

TSP is an adhesive plasma and extracellular matrix glycoprotein that mediates cell attachment, migration, and spreading, and plays a significant role in angiogenesis, wound healing, and phenotypic differentiation.³⁶ Sickle RBCs avidly bind purified, immobilized TSP under conditions of low shear flow *in vitro*.^{8,10,11} In addition,

soluble TSP enhances the adhesion of sickle RBCs to cultured endothelial cells and surface-bound TSP.^{10,11,37} We found that TSP-A10 inhibited sickle RBC adhesion to both immobilized purified TSP as well as to sickle RBCs bound to cytokine-activated endothelial cells in the presence of soluble TSP. Interestingly, we also found a baseline level of sickle RBC adhesion to cytokine-stimulated endothelial cells that was unaffected by scFv TSP-A10 as well as a marked increase in whole blood RBC adhesion to activated endothelial cells that was only partially inhibited by TSP-A10. These data emphasize the complexity of sickle RBC adhesion and confirm the theory that multiple adhesive pathways likely contribute to mediating sickle RBC adhesion in vivo. The fact that TSP-A10 significantly inhibited sickle RBC adhesion in the more complex system of activated endothelial cells and whole blood suggests a potentially physiologic role for sickle RBC–TSP–endothelial cell interactions in vivo. The inhibitory effect of TSP-A10 in the whole blood–endothelial cell system also compels further studies of this scFv using in vivo models of sickle cell disease.

TSP has multiple sites that mediate cell adhesion, including the amino-terminal heparin-binding domain,²⁶ sequences within the type 1 repeats that associate with CD36,³⁸ the Arg-Gly-Asp integrin-binding site within the last type 3 repeat of the calcium-binding domain,³⁹ and the carboxy-terminal TSP-CBD that binds to platelets and transformed cells.¹⁸ Using purified TSP proteolytic fragments, we have previously shown that the intact carboxy-terminal cell-binding and neighboring Ca⁺⁺-binding domains are required for TSP to recognize the sickle erythrocyte.¹⁵ Controlled chymotrypsin digestion that gradually cleaves the 140-kDa TSP fragment into the disulfide-linked 120-kDa TSP and 18-kDa fragments fully disrupted sickle RBC adhesion to surface-bound TSP in a dose-dependent manner. Since the carboxy-terminal 18-kDa fragment remains disulfide-linked to the 120-kDa fragment, the proteolytic cleavage likely destroys a critical conformational structure of the 18-kDa TSP fragment or the carboxy-terminal regions of the 120-kDa TSP fragment. That scFvs TSP-A10 and TSP-E9, which likely bind a similar region of TSP, also disrupt sickle RBC adhesion lends further support to the thesis that the carboxy-terminal regions of TSP, or the junction near the Ca⁺⁺-binding domain, and TSP-CBD are critical for RBC adhesion.

Integrin-associated protein (IAP or CD47) on endothelial cells, platelets, and transformed cell lines interacts with the carboxy-terminal TSP-CBD.^{40,41} Furthermore, the 4N1K peptide derived from the TSP-CBD has been shown to bind IAP and modify the adhesive phenotype of platelets and human melanoma cells via G protein–linked signaling pathways.⁴²⁻⁴⁴ In agreement with a role for the carboxy-terminus of TSP interacting with sickle RBCs, Brittain et al⁴⁵ have provided evidence that IAP on sickle RBCs, but not normal RBCs, binds surface-bound TSP. Additionally, the 4N1K peptide may also cause a modest¹⁵ or more striking³⁷ increase in

sickle RBC adhesion that varies with experimental conditions. Our finding that scFvs TSP-A10 and TSP-E9, which specifically bind the TSP Ca⁺⁺-binding domain or an adjacent portion of the TSP-CBD, significantly inhibit sickle RBC adhesion provides further evidence for an essential role of this region of TSP in the interaction of sickle RBCs with TSP. The effect of these scFvs may be due to either direct interference with a sickle RBC binding site or to changes induced in a critical conformational epitope(s) on TSP that is distal to the scFv binding site.

We have found that neither well-characterized adhesive peptide sequences from within the TSP cell-binding domain¹⁸ nor mAbs known to block cellular binding to the TSP cell-binding domain¹⁶ inhibit sickle RBC adhesion to TSP within our experimental model.¹⁵ Thus, the site, or sites, on TSP that recognizes the sickle RBC appears to be a novel adhesive site within the cell-binding domain, or a distant site on TSP affected by the conformation of the cell-binding domain. The lack of adhesive TSP peptides or mAbs that bind TSP-CBD and inhibit sickle RBC binding to immobilized TSP has greatly limited studies to further define sickle RBC–adhesive ligand interactions. Therefore, the successful selection of several unique scFvs that selectively bind TSP and affect sickle RBC adhesion will provide tools to improve our understanding of sickle RBC adhesion. The use of these scFvs in such studies may be facilitated by improving their affinities by reducing the off rates using in vitro affinity maturation techniques such as light-chain shuffling, mutagenesis, or CDR3 randomization.⁴⁶⁻⁴⁹ The V genes encoding such affinity-matured antibodies may then be recloned as an IgG with modified heavy chain constant domains to produce a TSP blocking antibody that does not activate complement or bind Fc receptors.⁵⁰

Sickle RBC adhesion to the vascular endothelium likely contributes to the pathogenesis of vascular obstruction in sickle cell disease. Characterization of sickle RBC interactions with the vascular endothelium and extracellular matrix will improve our understanding of vaso-occlusive events in sickle cell disease and should provide insight as to mechanisms that will inhibit the adhesion of the sickle RBC to the vessel wall and prevent endothelial injury and, therefore, subsequent vascular obstruction. These newly identified antibodies will be novel reagents to further investigate functional characteristics of sickle RBC interactions with TSP, including the role of TSP in experimental models of sickle cell vaso-occlusion.

Acknowledgments

We would like to thank Evelyn Brown and Gwendolyn Lea for their assistance for recruiting patients and obtaining blood samples for this study. We would also like to thank Sandra Holzman for her assistance with the TSP digestions and immunoblot analyses.

References

1. Hebbel RP. Beyond hemoglobin polymerization: the red blood cell membrane and sickle disease pathophysiology. *Blood*. 1991;77:214-237.
2. Hebbel RP, Yamada O, Moldow CF, Jacob HS, White JG, Eaton JW. Abnormal adherence of sickle erythrocytes to cultured vascular endothelium: possible mechanism for microvascular occlusion in sickle cell disease. *J Clin Invest*. 1980; 65:154-160.
3. Mohandas N, Evans E. Sickle erythrocyte adherence to vascular endothelium: morphologic correlates and the requirement for divalent cations and collagen-binding plasma proteins. *J Clin Invest*. 1985;76:1605-1612.
4. Barabino GA, McIntire LV, Eskin SG, Sears DA, Udden M. Endothelial cell interactions with sickle cell, sickle trait, mechanically injured, and normal erythrocytes under controlled flow. *Blood*. 1987; 70:152-157.
5. Kaul DK, Fabry ME, Nagel RL. Microvascular sites and characteristics of sickle cell adhesion to vascular endothelium in shear flow conditions: pathophysiological implications. *Proc Natl Acad Sci U S A*. 1989;86:3356-3360.
6. French JA II, Kenny D, Scott JP, et al. Mechanisms of stroke in sickle cell disease: sickle erythrocytes decrease cerebral blood flow in rats after nitric oxide synthase inhibition. *Blood*. 1997;89: 4591-4599.
7. Kaul DK, Fabry ME, Costantini F, Rubin EM, Nagel RL. In vivo demonstration of red cell-endothelial interaction, sickling and altered microvascular response to oxygen in the sickle transgenic mouse. *J Clin Invest*. 1995;96:2845-2853.
8. Hillery CA, Du MC, Montgomery RR, Scott JP. Increased adhesion of erythrocytes to components of the extracellular matrix: isolation and

- characterization of a red blood cell lipid that binds thrombospondin and laminin. *Blood*. 1996;87:4879-4886.
9. Joneckis CC, Shock DD, Cunningham ML, Orringer EP, Parise LV. Glycoprotein IV-independent adhesion of sickle red blood cells to immobilized thrombospondin under flow conditions. *Blood*. 1996;87:4862-4870.
 10. Sugihara K, Sugihara T, Mohandas N, Hebbel SP. Thrombospondin mediates adherence of CD36+ sickle reticulocytes to endothelial cells. *Blood*. 1992;80:2634-2642.
 11. Brittain HA, Eckman JR, Swerlick RA, Howard RJ, Wick TM. Thrombospondin from activated platelets promotes sickle erythrocyte adherence to human microvascular endothelium under physiologic flow: a potential role for platelet activation in sickle cell vaso-occlusion. *Blood*. 1993;81:2137-2143.
 12. Manodori AB, Barabino GA, Lubin BH, Kuypers FA. Adherence of phosphatidylserine-exposing erythrocytes to endothelial matrix thrombospondin. *Blood*. 2000;95:1293-1300.
 13. Barabino GA, Liu XD, Ewenstein BM, Kaul DK. Anionic polysaccharides inhibit adhesion of sickle erythrocytes to the vascular endothelium and result in improved hemodynamic behavior. *Blood*. 1999;93:1422-1429.
 14. Browne PV, Mosher DF, Steinberg MH, Hebbel RP. Disturbance of plasma and platelet thrombospondin levels in sickle cell disease. *Am J Hematol*. 1996;51:296-301.
 15. Hillery CA, Scott JP, Du MC. The carboxy-terminal cell-binding domain of thrombospondin is essential for sickle red blood cell adhesion. *Blood*. 1999;94:302-309.
 16. Kosfeld MD, Pavlopoulos TV, Frazier WA. Cell attachment activity of the carboxyl-terminal domain of human thrombospondin expressed in *Escherichia coli*. *J Biol Chem*. 1991;266:24257-24259.
 17. Dixit VM, Haverstick DM, O'Rourke KM, et al. A monoclonal antibody against human thrombospondin inhibits platelet aggregation. *Proc Natl Acad Sci U S A*. 1985;82:3472-3476.
 18. Kosfeld MD, Frazier WA. Identification of a new cell adhesion motif in two homologous peptides from the COOH-terminal cell binding domain of human thrombospondin. *J Biol Chem*. 1993;268:8808-8814.
 19. Winter G, Griffiths AD, Hawkins RE, Hoogenboom HR. Making antibodies by phage display technology. *Annu Rev Immunol*. 1994;12:433-455.
 20. Griffiths AD, Williams SC, Hartley O, et al. Isolation of high affinity human antibodies directly from large synthetic repertoires. *EMBO J*. 1994;13:3245-3260.
 21. Hoogenboom HR, Griffiths AD, Johnson KS, Chiswell DJ, Hudson P, Winter G. Multi-subunit proteins on the surface of filamentous phage: methodologies for displaying antibody (Fab) heavy and light chains. *Nucleic Acids Res*. 1991;19:4133-4137.
 22. Marks JD, Hoogenboom HR, Bonnett TP, McCafferty J, Griffiths AD, Winter G. By-passing immunization: human antibodies from V-gene libraries displayed on phage. *J Mol Biol*. 1991;222:581-597.
 23. Slayter HS. Secretion of thrombospondin from human blood platelets. *Methods Enzymol*. 1989;169:251-268.
 24. Evan GI, Lewis GK, Ramsay G, Bishop JM. Isolation of monoclonal antibodies specific for human c-myc proto-oncogene product. *Mol Cell Biol*. 1985;5:3610-3616.
 25. Cook GP, Tomlinson IM. The human immunoglobulin VH repertoire. *Immunol Today*. 1995;16:237-242.
 26. Dixit VM, Grant GA, Santoro SA, Frazier WA. Isolation and characterization of a heparin-binding domain from the amino terminus of platelet thrombospondin. *J Biol Chem*. 1984;259:10100-10105.
 27. Galvin NJ, Vance PM, Dixit VM, Fink B, Frazier WA. Interaction of human thrombospondin with types I-V collagen: direct binding and electron microscopy. *J Cell Biol*. 1987;104:1413-1422.
 28. Prater CA, Plotkin J, Jaye D, Frazier WA. The propeptide-like type I repeats of human thrombospondin contain a cell attachment site. *J Cell Biol*. 1991;112:1031-1040.
 29. Jaffe EA, Nachman RL, Becker CG, Minick CR. Culture of human endothelial cells derived from umbilical veins. *J Clin Invest*. 1973;52:2745-2756.
 30. Swerlick RA, Eckman JR, Kumar A, Jeitler M, Wick TM. $\alpha 4\beta 1$ -integrin expression on sickle reticulocytes: vascular cell adhesion molecule-1-dependent binding to endothelium. *Blood*. 1993;82:1891-1899.
 31. Natarajan M, Udden MM, McIntire LV. Adhesion of sickle red blood cells and damage to interleukin-1 beta stimulated endothelial cells under flow in vitro. *Blood*. 1996;87:4845-4852.
 32. Shiu YT, Udden MM, McIntire LV. Perfusion with sickle erythrocytes up-regulates ICAM-1 and VCAM-1 gene expression in cultured human endothelial cells. *Blood*. 2000;95:3232-3241.
 33. Galvin NJ, Dixit VM, O'Rourke KM, Santoro SA, Grant GA, Frazier WA. Mapping of epitopes for monoclonal antibodies against human platelet thrombospondin with electron microscopy and high sensitivity amino acid sequencing. *J Cell Biol*. 1985;101:1434-1441.
 34. Fabry ME, Rajanayagam V, Fine E, et al. Modeling sickle cell vasoocclusion in the rat leg: quantification of trapped sickle cells and correlation with 31P metabolic and 1H magnetic resonance imaging changes. *Proc Natl Acad Sci U S A*. 1989;86:3808-3812.
 35. Hughes-Jones NC, Bye JM, Gorick BD, Marks JD, Ouweland WH. Synthesis of Rh Fv phage-antibodies using VH and VL germline genes. *Br J Haematol*. 1999;105:811-816.
 36. Santoro SA, Frazier WA. Isolation and characterization of thrombospondin. *Methods Enzymol*. 1987;144:438-446.
 37. Brittain JE, Mlinar KJ, Anderson CS, Orringer EP, Parise LV. Activation of sickle red blood cell adhesion via integrin-associated protein/CD47-induced signal transduction. *J Clin Invest*. 2001;107:1555-1562.
 38. Asch AS, Silbiger S, Heimer E, Nachman RL. Thrombospondin sequence motif (CSVTCG) is responsible for CD36 binding. *Biochem Biophys Res Commun*. 1992;182:1208-1217.
 39. Lawler J, Weinstein R, Hynes RO. Cell attachment to thrombospondin: the role of ARG-GLY-ASP, calcium, and integrin receptors. *J Cell Biol*. 1988;107:2351-2361.
 40. Gao AG, Frazier WA. Identification of a receptor candidate for the carboxyl-terminal cell binding domain of thrombospondins. *J Biol Chem*. 1994;269:29650-29657.
 41. Gao AG, Lindberg FP, Finn MB, Blystone SD, Brown EJ, Frazier WA. Integrin-associated protein is a receptor for the C-terminal domain of thrombospondin. *J Biol Chem*. 1996;271:21-24.
 42. Gao AG, Lindberg FP, Dimitry JM, Brown EJ, Frazier WA. Thrombospondin modulates alpha v beta 3 function through integrin-associated protein. *J Cell Biol*. 1996;135:533-544.
 43. Chung J, Gao AG, Frazier WA. Thrombospondin acts via integrin-associated protein to activate the platelet integrin $\alpha 5\beta 1$. *J Biol Chem*. 1997;272:14740-14746.
 44. Frazier WA, Gao AG, Dimitry J, et al. The thrombospondin receptor integrin-associated protein (CD47) functionally couples to heterotrimeric Gi. *J Biol Chem*. 1999;274:8554-8560.
 45. Brittain JE, Mlinar KJ, Anderson CS, Orringer EP, Parise LV. Integrin-associated protein is an adhesion receptor on sickle red blood cells for immobilized thrombospondin. *Blood*. 2001;97:2159-2164.
 46. Irving RA, Kortt AA, Hudson PJ. Affinity maturation of recombinant antibodies using *E. coli* mutator cells. *Immunotechnology*. 1996;2:127-143.
 47. Schier R, Bye J, Apell G, et al. Isolation of high-affinity monomeric human anti-c-erbB-2 single chain Fv using affinity-driven selection. *J Mol Biol*. 1996;255:28-43.
 48. Schier R, McCall A, Adams GP, et al. Isolation of picomolar affinity anti-c-erbB-2 single-chain Fv by molecular evolution of the complementarity determining regions in the center of the antibody binding site. *J Mol Biol*. 1996;263:551-567.
 49. Kjaer S, Wind T, Ravn P, Ostergaard M, Clark BF, Nissim A. Generation and epitope mapping of high-affinity scFv to eukaryotic elongation factor 1A by dual application of phage display. *Eur J Biochem*. 2001;268:3407-3415.
 50. Armour KL, Clark MR, Hadley AG, Williamson LM. Recombinant human IgG molecules lacking Fc gamma receptor I binding and monocyte triggering activities. *Eur J Immunol*. 1999;29:2613-2624.
 51. Kabat EA, Wu TT, Reid-Miller M, Perry HM, Gottesmann KS. Sequences of proteins of immunological interest. Bethesda, MD: NIH; 1991.